DOI 10.24425/aee.2024.150893

Moving-fuzzy sliding mode control of aircraft wing-rock motion

SINDA ALOUI [1], SAMIA LARGUECH [2]✉, SHABANA UROOJ [2], NORAH ALWADAI [3]

[1] *Laboratory of Sciences and Techniques of Automatic control computer engineering (Lab-STA)*
National School of Engineering of Sfax, University of Sfax
Postal Box 1173, 3038 Sfax, Tunisia

[2] *Department of Electrical Engineering, College of Engineering*
Princess Nourah bint Abdulrahman University
Riyadh, Saudi Arabia

[3] *Department of Physics, College of Sciences,*
Princess Nourah bint Abdulrahman University,
Riyadh, Saudi Arabia

e-mail: sinda.aloui@enis.tn, {✉ SRLarguech/SMUrooj/nmAlWadai}@pnu.edu.sa

(Received: 06.02.2024, revised: 23.08.2024)

Abstract: This work represents a moving fuzzy sliding mode controller (SMC) to suppress the wing-rock motion, a self-sustaining cycle oscillation caused by the nonlinear coupling between the unsteady aerodynamic forces and the dynamic response of the aircraft. Based on fuzzy systems, a moving algorithm is designed to estimate the unknown nonlinear dynamic function of the system in the control topology. The fuzzy algorithm is formulated by taking the width's value, and based on Lyapunov theory, the membership function's mean vector is adapted online. Simulation results, for examples that include small and large initial conditions, demonstrate the effectiveness of the proposed fuzzy sliding mode controller.

Key words: adaptive sliding mode control, moving fuzzy system, wing-rock motion

1. Introduction

To operate effectively at high angles of attack and inside slips, high-performance aircraft must meet specific mission requirements. However, achieving track accuracy and maximum angle of attack during operational maneuvers presents challenges, notably in addressing wing roll. This phenomenon can befuddle pilots and severely hinder aircraft combat effectiveness, potentially compromising safety during takeoff and landing. Predicting the frequency and amplitude of limiting cycle oscillations and comprehending the dynamics of wing-rock motion (WRM) has garnered significant attention. Various studies [1–6] have tackled these issues. A theoretical model for nonlinear rolling motion was developed using simple differential equations. Subsequently, numerous control methods have been proposed, including adaptive control techniques, robust $H\infty$ control, and output feedback linearization [7–12].

The authors in [13], provide a detailed description of methods for adaptive control design, utilizing both classical and neural network-based approaches to effectively stabilize oscillatory motion of Aircraft Wing Rock by adapting to uncertainties.

In [14], the concept of adaptive control for feedback linearizable systems is employed in devising a control strategy for managing wing rock motion, with an extension of the technique to incorporate tracking capabilities.

Although these methods give satisfactory results in terms of accuracy, they directly rely on complex and uncertain mathematical models of wing rock motion. To overcome this issue related to different non-linear systems, there exist many important works lie ahead including fuzzy set theory [15–18]. Since it is a model-free design method [19, 20].

In the literature, several research studies have dealt with the robustness of controllers with respect to the model uncertainties and external disturbance. In fact, in [21] a systematic move blocking-based robust model predictive control for nonlinear systems due to the model uncertainties and disturbances based on Takagi–Sugeno fuzzy models is provided. In [22], a data-driven-based disturbance observer is presented. In [23], fuzzy sliding mode control for turbocharged diesel engine is developed in order to reduce the effect of the external disturbance. In [24], a fuzzy-model-based approach is developed to investigate the reinforcement learning-based optimization for nonlinear Markov jump singularly perturbed systems.

This study introduces a dynamic fuzzy sliding mode controller (SMC) aimed at mitigating wing-rock motion, a cyclic oscillation phenomenon resulting from the nonlinear interaction between unsteady aerodynamic forces and the aircraft's dynamic response. Utilizing fuzzy systems, a dynamic algorithm is devised to estimate the unknown nonlinear dynamic function of the system within the control framework. In fact, the parameters of the fuzzy logic systems were fixed arbitrary, thus leading to many possibilities for FLSs. In this paper, the moving fuzzy approach is used on the one hand to improve the quality of fuzzy approximation, and on the other hand when we do not have a rigorous description of the evolution of the system to deduce the most appropriate membership function. The aircraft wing sweep motion is described and modeled in Section 2 of this paper. In Section 3, we introduce the mobile fuzzy logic system. To demonstrate the control strategy's efficacy, simulations results are presented in Section 4 presents simulation. In Section 5, a comparative study is presented to demonstrate the effectiveness of the proposed approach. Finally, Section 6 summarizes the main work carried out in this paper.

2. Problem statement and dynamic model

To formulate the state equations of the WRM system, consider the following dynamic equations:

$$\begin{aligned} \dot{x}_1 &= x_2, \\ \dot{x}_2 &= f(x_1, x_2) + u + d(t), \end{aligned} \tag{1}$$

where: u is the control input, $x = [x_1, x_2] = [\varphi, \dot{\varphi}]$ is the state vector, $d(t)$ is the external bounded disturbance where $|d(t)| \leq \beta$, $\beta \geq 0$.

$f(x_1, x_2)$ is an unknown bounded function defined as:

$$f(x_1, x_2) = -\omega^2\varphi + \mu_1\dot{\varphi} + b_2\dot{\varphi}^3 + \mu_2\varphi^2\dot{\varphi} + b_2\dot{\varphi}^2\varphi \ , \tag{2}$$

where: $\omega^2 = -Ca_1, \mu_1 = Ca_2 - D, \mu_2 = Ca_4, b_1 = Ca_3, b_2 = Ca_5$ and $C = \rho U_\infty Sb/2I_{xx}$ is fixed constant, $C = 0.354$.

Given in Table 1, aerodynamic parameters $a_1, \ldots, a_5$ are nonlinear functions of the angle of attack α.

A state vector is required to follow a desired trajectory $x_d = [x_{d1}, \dot{x}_{d2}]^T = [\varphi_d, \dot{\varphi}_d]^T$ under the constraint that all relevant signals must be bound by the input law.

Table 1. Aerodynamic parameters

α	a_1	a_2	a_3	a_4	a_5
15	–0.01026	–0.02117	–0.14181	0.99735	–0.83478
20	–0.05686	0.03254	0.07334	–0.05970	1.4681

3. Robust moving fuzzy controller design

3.1. Step 1: Approximation of $f(x_1, x_2)$

For an aircraft WRM system, the motion dynamic $f(x_1, x_2)$ is perturbed or unknown. As a result, putting the conventional sliding mode controller into action is challenging. To circumvent this problem, a fuzzy logic system can be used. A moving fuzzy logic system will be developed in this work. For this approach, not only the system parameter vectors are adjusted online (case of fuzzy logic system) but also the width and the center vectors of the membership functions. All the adaptive laws are deduced based on Lyapunov theory.

First, a short description of adaptive fuzzy logic (AFL) systems is provided in the following section to help distinguish the proposed strategy from the adaptive fuzzy logic system. Second, we demonstrated a system of moving fuzzy logic.

3.1.1. Fuzzy logic system (FLS) description

The four parts of an FLS are as follows: knowledge base, fuzzy inference engine that uses fuzzy rules and defuzzifier. In the rest of the paper, an FLS as shown in Fig. 1, is incorporated in the control law to estimate the dynamics of the wing-rock system independently of the attack angle α.

According to the universal approximation theorem, uniformly over a compact set, the FLS may evenly and accurately estimate any nonlinear function [1, 16].

A mapping is carried out by a multi-input single-output (MISO) FLS from an input vector $x = [x_1, x_2, \ldots x_n]^T \in \mathrm{R}^n$ to an output variable $z \in \mathrm{R}$.

With central average defuzzification, the output of the FLS is communicated as:

$$z = \theta^T \xi(x), \tag{3}$$

where: $\xi = [\xi_1, \xi_2, \ldots, \xi_N]^T$ is a set of fuzzy basis functions, $\theta^T = [\theta_1, \theta_2 \ldots, \theta_N]$ is a vector grouping all consequent parameters.

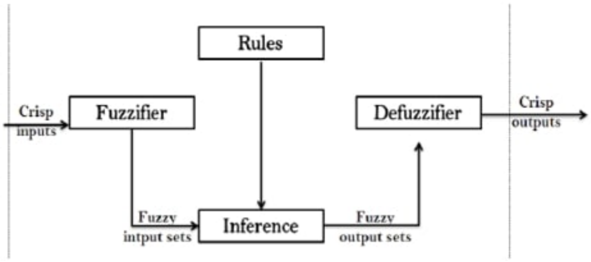

Fig. 1. Fuzzy logic system block diagram

$\xi^k(x)$ is defined by:

$$\xi^k(x) = \frac{\prod_{i=1}^{n} \mu_{A_i^k}(x_i)}{\sum_{k=1}^{N}\left(\prod_{i=1}^{n} \mu_{A_i^k}(x_i)\right)}, \tag{4}$$

where: $u^k_{A_i^l}(x_i)$ is the membership function which represents the fuzzy meaning of the symbol A_i^k, $i = 1, \ldots, n$, $k = 1, \ldots, N$, N is the total number of rules.

Fuzzy logic system $\hat{f}(x)$ approximates $f(x)$ and it is obtained by:

$$\hat{f}(x) = \theta_f^T \xi(x), \tag{5}$$

where: $\xi(x)$ represents the fuzzy basis vector.

θ_f is the corresponding adjustable parameter vector, where θ_f is tuned on-line.

Adaptive law is used to adjust the vectors of the system parameters θ_f :

$$\dot{\theta}_f = \gamma_f s\xi, \tag{6}$$

where: γ_f is the positive constant and s is the sliding surface, we will be detailed later.

3.1.2. Moving fuzzy logic systems description

The highlights of this approach consist of reducing the number of fuzzy rules used to approximate the motion dynamic $f(x_1, x_2)$ while guaranteeing a good approximation (a low fuzzy approximation error).

The following can be used to rewrite the output of the fuzzy logic system with central average defuzzification (3), [20, 23]:

$$z = \theta^T \xi(x, \sigma, \delta), \tag{7}$$

where: $\xi = [\xi_1, \xi_2, \ldots, \xi_N]^T$ is a set of fuzzy basis functions, $\theta^T = [\theta_1, \theta_2 \ldots, \theta_N]$ is a vector gathering every consequent parameters, δ and σ are width and center vectors of the membership functions, respectively.

ξ is defined in this case by:

$$\xi^k(x,\sigma,\delta) = \frac{\prod_{i=1}^{n} \mu_{A_i^k}(x_i,\sigma_k,\delta_k)}{\sum_{k=1}^{N}\left(\prod_{i=1}^{n} \mu_{A_i^k}(x_i,\sigma_k,\delta_k)\right)}, \tag{8}$$

where: $\mu^k_{A_i^k}(x_i)$ is the membership function that depicts the symbol's fuzzy meaning A_i^k, $k = 1,\ldots,N$, N is the total number of rules and, while δ, σ are the width and center vectors of the membership functions.

Fuzzy logic system $\hat{f}(x,\sigma,\delta)$ approximate $f(x_1,x_2)$ is obtained by:

$$\hat{f}(x,\sigma,\delta) = \theta_f^T \xi(x,\sigma,\delta), \tag{9}$$

where: $\xi(x,\sigma,\delta)$ represents the fuzzy basis vector and θ_f is the corresponding adjustable parameter vector, θ_f is tuned on-line.

The following adaptive laws are utilized to adjust the system parameter vectors θ_f, σ and δ.

$$\dot{\theta}_f = \gamma_f s\left(\xi - \xi_\alpha \sigma - \xi_\delta \delta\right), \tag{10}$$

$$\dot{\sigma} = \gamma_\sigma s \xi_\sigma^T(\theta_f), \tag{11}$$

$$\dot{\delta} = \gamma_\delta s \xi_\delta^T(\theta_f), \tag{12}$$

where: γ_f, γ_σ and γ_δ are positive constants.

3.2. Step 2: Moving fuzzy SMC design

Tracking error vector is defined as:

$$e = [e_1, \dot{e}_1] = [e_1, e_2], \tag{13}$$

where: $e_i = x_i - x_{id}$, $i = 1,2$, x_{id} are the desired reference trajectory of the outputs.

Sliding surface of the system (1) is given by:

$$s = k_1 e_2 + k_2 e_1, \tag{14}$$

where: k_1 and k_2 are positive constants chosen such that all roots $s^2 + k_1 s + k_2 = 0$ are located in the complex plane's left side.

Considering time derivative of the sliding surface:

$$\begin{gathered} \dot{s} = k_1 \dot{e}_2 + k_2 \dot{e}_1, \\ \dot{s} = k_1\left[f(x_1,x_2) + u - \dot{x}_{d_2}\right] + k_2 e_2, \end{gathered} \tag{15}$$

where: x_d is the vector of desired trajectories.

The equation that follows provides the sliding mode control law:

$$u = u_{eq} + u_{sw}, \tag{16}$$

where: u_{eq} is the equivalent control law calculated by $\dot{s} = 0$ as:

$$u_{eq} = -f(x_1, x_2) - \frac{k_2}{k_1}e_2 + \dot{x}_{d_2}, \tag{17}$$

and u_{sw} is the discontinuous control law defined by:

$$u_{sw} = \tau \text{sign}(s). \tag{18}$$

The chattering phenomenon, which has the ability to excite high-frequency dynamics, is caused by the existence of the signum function in the switching term in the traditional sliding mode technique. To avoid this problem, in [25], the fuzzy disturbance observer is developed to estimate the mismatched disturbance. In this paper an adaptive PI term is used. In fact, the integral term when added to the proportional term accelerates the movement of the process towards the set point and eliminates the residual steady-state error that occurs with a proportional term.

Adaptive PI term is defined as follows:

$$u_{\text{PI}}(s) = \rho(s|\Theta_{\text{PI}}) = \Theta_{\text{PI}}^T \Psi(s), \tag{19}$$

where: $\Theta_{\text{PI}}^T = \left[k_p, k_i\right]^T$ is the adaption gain vector and $\Psi(s) = \left[s, \int s\text{d}t\right]^T$ are regressive vectors. k_p and k_i are the control gains adjusted online from an adaptive law.

Combining the moving fuzzy logic system with the sliding mode controller and PI switching law, the resulted control law becomes:

$$u = -\hat{f}(x, \sigma, \delta) - \frac{k_2}{k_1}e_2 + \dot{x}_{d_2} - u_{\text{PI}}(s), \tag{20}$$

where the system function is presented by (9).

Moreover, the PI adaption gain vector is adjusted by the following adaptive law:

$$\dot{\Theta}_{\text{PI}} = \gamma_{\text{PI}} s \Psi(s), \tag{21}$$

where γ_{PI} is a positive constant.

Theorem:

Consider a wing rock system defined as (1), *and the system function* $\hat{f}(x)$ *is given by* (5), *adaptive fuzzy sliding mode control law* (20), *the* u_{PI} *controller is defined as* (19) *and the parameters vector* θ_f, α, δ *and* Θ_{PI} *are adjusted by adaptive laws* (10), (11), (12), *and* (21) *ensures the tracking errors converge to zero asymptotically and that all the closed loop signals are bounded.*

Proof:

First, let us define the following variables:

$$\Theta_{\text{PI}}^* = \arg \min_{|\theta_{\text{PI}}| \in \Omega_{\text{PI}}} [\sup_{|s| \in R^n} ||\rho(s|\Theta_{\text{PI}}) - \eta \text{sgn}(s)||], \tag{22}$$

where: $\eta\text{sgn}(s)$ is the discontinuous term of the conventional sliding mode control with the signum function "sign" such $\eta > D$ and Ω_{PI} denotes the set of the suitable bounds on Θ_{PI}
and

$$\Omega_\rho = \left\{\Theta_{\text{PI}} \in R^2 : ||\Theta_{\text{PI}}|| < M_\rho\right\}. \tag{23}$$

Denote:

$$W_{\mathrm{PI}}= \rho(s|\Theta^*_{\mathrm{PI}}) - \eta \mathrm{sgn}(s). \tag{24}$$

The approximation error W_{PI} belongs to $L_2[0;t], \forall t \in [0,\infty)$.

Define the optimal parameters vectors can be represented as:

$$\begin{aligned}
\theta_f^* &= \arg \min_{|\theta_f|\in\Omega_f} [\sup_{|x|\in\Omega_x} |\hat{f}(x,\sigma,\delta) - f(x_1,x_2)|,\\
\sigma^* &= \arg \min_{|\alpha|\in\Omega_\alpha} [\sup_{|x|\in\Omega_x} |\hat{f}(x,\sigma,\delta) - f(x_1,x_2)|,\\
\delta^* &= \arg \min_{|\theta_\beta|\in\Omega_\beta} [\sup_{|x|\in\Omega_x} |\hat{f}(x,\sigma,\delta) - f(x_1,x_2)|,
\end{aligned}$$

where: Ω_f, Ω_σ, Ω_δ denote the sets of suitable bounds on $\theta_f \sigma, \delta$, respectively, and Ω_x denotes the set of the suitable bounds on x.

Assume that the constraint sets $\Omega_f, \Omega_\sigma \Omega_\delta$ are specified as:

$$\begin{aligned}
\Omega_f &= \left\{\theta_f : \left\|\theta_f\right\| < M_f\right\},\\
\Omega_\sigma &= \{\sigma : ||\sigma|| < M_\sigma\},\\
\Omega_\delta &= \{\delta : ||\delta|| < M_\delta\}.
\end{aligned}$$

Consider the following Lyapunov function:

$$V = \frac{1}{2}s^2 + \frac{1}{2\gamma_f}\widetilde{\theta}_f^T\widetilde{\theta}_f + \frac{1}{2\gamma_\sigma}\widetilde{\sigma}^T\widetilde{\sigma} + \frac{1}{2\gamma_\delta}\widetilde{\delta}^T\widetilde{\delta} + \frac{1}{2\gamma_{\mathrm{PI}}}\widetilde{\Theta}_{\mathrm{PI}}^T\widetilde{\Theta}_{\mathrm{PI}}. \tag{25}$$

If the time derivative of the Lyapunov function is negative, the system must be stable.

$$\dot{V} = s\dot{s} + \frac{1}{\gamma_f}\widetilde{\theta}_f^T\dot{\theta}_f + \frac{1}{2\gamma_\sigma}\widetilde{\sigma}^T\dot{\sigma} + \frac{1}{2\gamma_\delta}\widetilde{\delta}^T\dot{\delta} + \frac{1}{2\gamma_{\mathrm{PI}}}\widetilde{\Theta}_{\mathrm{PI}}^T\dot{\Theta}_{\mathrm{PI}}. \tag{26}$$

If we substitute (20) into (15), we obtain:

$$\dot{s}(x) = k_1\left[f(x_1,x_2) - f(x,\sigma,\delta)\right] - k_1 U_{\mathrm{PI}} + k_1 d(t). \tag{27}$$

By adding and substituting $\rho(s|\Theta^*_{\mathrm{PI}})$, (24) can be rewritten as:

$$\dot{s}(x) = k_1\left[f(x_1,x_2) - f(x,\sigma,\delta)\right] - k_1\widetilde{\Theta}_{\mathrm{PI}}^T\Psi(s) - k_1\eta\mathrm{sgn}(s) + k_1(W_{\mathrm{PI}} + d(t)). \tag{28}$$

If we consider the double Taylor expansion for system $f(x,\sigma,\delta)$ described as:

$$f(x,\alpha,\delta) - f(x_1,x_2) = \widetilde{\theta}_f^T\left[\xi - \xi_\alpha\sigma - \xi_\delta\delta\right] + \theta_f^T\left[\xi_\alpha\widetilde{\sigma} + \xi_\delta\widetilde{\delta}\right] + w_f, \tag{29}$$

where:

$$\begin{aligned}
&\widetilde{\theta}_f = \theta_f - \theta_f^*, \quad \widetilde{\sigma} = \sigma - \sigma^*, \quad \widetilde{\delta} = \delta - \delta^*, \quad \xi = \xi(x,\sigma,\delta), \quad \xi_\alpha = \xi_\alpha(x,\sigma,\delta),\\
&\xi_\delta = \xi_\delta(x,\sigma,\delta), \quad w_f = \widetilde{\theta}_f^T\left[\xi_\alpha\sigma^* + \xi_\delta\delta^*\right] + \left[f(x,\sigma^*,\delta^*) - f(x_1,x_2)\right].
\end{aligned}$$

Now, Eq. (26) can be written as follows:

$$\dot{V} = k_1 \left(\widetilde{\theta}_f^T [\xi - \xi_\sigma \sigma - \xi_\delta \delta] + \theta_f^T [\xi_\sigma \widetilde{\sigma} - \xi_\delta \widetilde{\delta}] + w_f - \widetilde{\Theta}_{\mathrm{PI}}^T \Psi(s) - \eta \mathrm{sgn}(s) + W_{\mathrm{PI}}\right) + \\ + k_1 d(t) + \frac{1}{\gamma_f} \widetilde{\theta}_f^T \dot{\theta}_f + \frac{1}{\gamma_\sigma} \widetilde{\sigma}^T \dot{\sigma} + \frac{1}{\gamma_\delta} \widetilde{\delta}^T \dot{\delta} + \frac{1}{\gamma_{\mathrm{PI\,PI}}} \widetilde{\Theta}^T \dot{\Theta}_{\mathrm{PI}} \tag{30}$$

and $W_{\max} = w_f + W_{\mathrm{PI}}$.

$$\dot{V} \le \widetilde{\theta} f^T (k_1 s[\xi - \xi_\sigma \sigma - \xi_\delta \delta + \frac{1}{\gamma_f} \dot{\theta}_f] + \widetilde{\sigma}^T [-k_1 \xi_\sigma^T \theta_f + \frac{1}{\gamma_\sigma} \dot{\sigma}] + \widetilde{\delta}^T [-k_1 \xi_\delta^T \theta_f + \frac{1}{\gamma_\delta} \dot{\delta}] + \\ + \widetilde{\Theta}_{\mathrm{PI}}^T [k_1 s \Psi(s) - \frac{1}{\gamma_{\mathrm{PI}}} \dot{\Theta}_{\mathrm{PI}}] + k_1 s D + k_1 s W_{\max} - k_1 \eta \mathrm{sgn}(s). \tag{31}$$

When the adaptation rules (10), (11), (12) and (21) are substituted in (31) we get:

$$\dot{V} < -k_1 \eta \, |s| + |s| \, (W_{\max} + D), \\ \dot{V} < -k_1 \eta \, |s| < 0 \; \eta > W_{\max} + D. \tag{32}$$

In addition, it can be demonstrated from (32) that the closed-loop system's robustness and semi-global asymptotic stability are guaranteed and tracking errors converge asymptotically converge to zero It is assumed that all parameter vectors fall within the constraint sets to achieve global stability. The adaptive laws (10), (11), (12) and (21) can be modified with the projection algorithm (Guo, Luo and Bao, 2022) to ensure that the parameters are bound.

4. Simulation results

Using the following example, we validate the effectiveness of the moving fuzzy sliding mode controller on the tracking control of an aircraft wing-rock motion.

Table 1 lists the delta wing's aerodynamic properties for simulations at 15° and 25° angles of attack.

Control parameters are selected as: $\gamma_{\mathrm{PI}} = 0.3$, $k_1 = 1$, $k_2 = 60$, $M_f = 10$.

The selected reference trajectory vector is $[\phi(0)\, \dot{\phi}(0)]^T = [\sin(t) \cos(t)]^T$, the external perturbation is $\mathrm{d}(t) = \cos(10t)$.

We select membership functions that approximate the nonlinear function $f(x_1, x_2)$.

A 2^2 potential combination should be found in order to cover the controllability zone.

The efficiency of the suggested control techniques is examined using two initial conditions for the state vector: a small initial condition and a large one.

$\phi(0) = 103.14°$, $\dot{\phi}(0) = 57.3°/s$: large initial condition,

$\phi(0) = 11.46°$, $\dot{\phi}(0) = 2.865°/s$: small initial condition.

4.1. Case 1: a small initial condition

Figures 2 to 9 show the simulation results for the suggested controller.

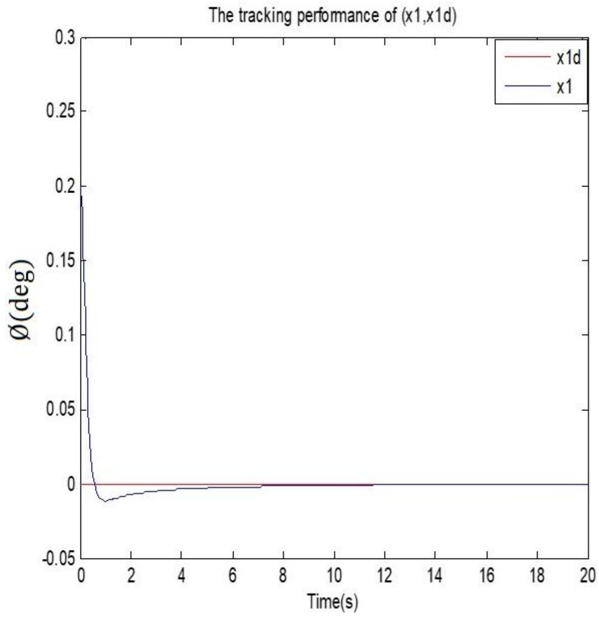

Fig. 2. Roll angle response

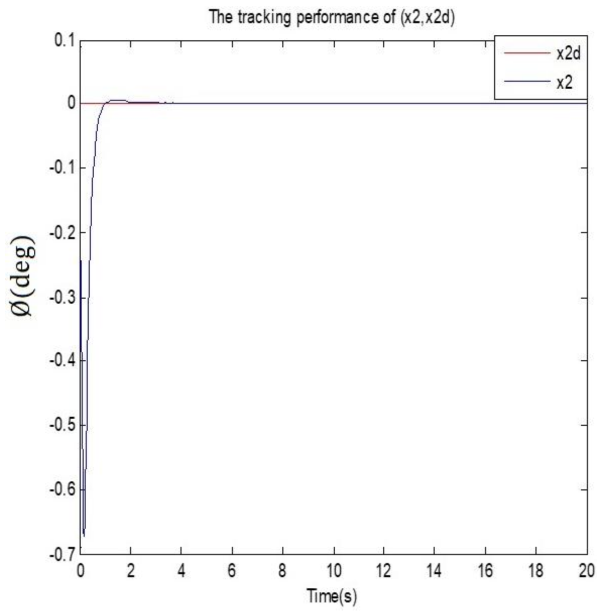

Fig. 3. Roll rate response

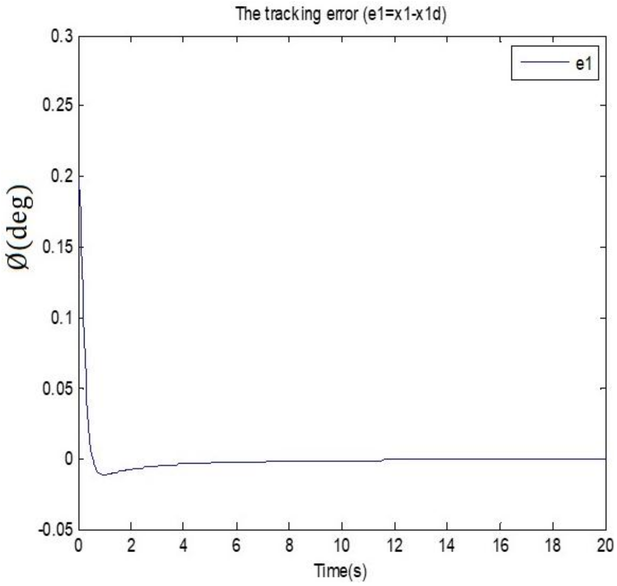

Fig. 4. Tracking errors e_1 evolution

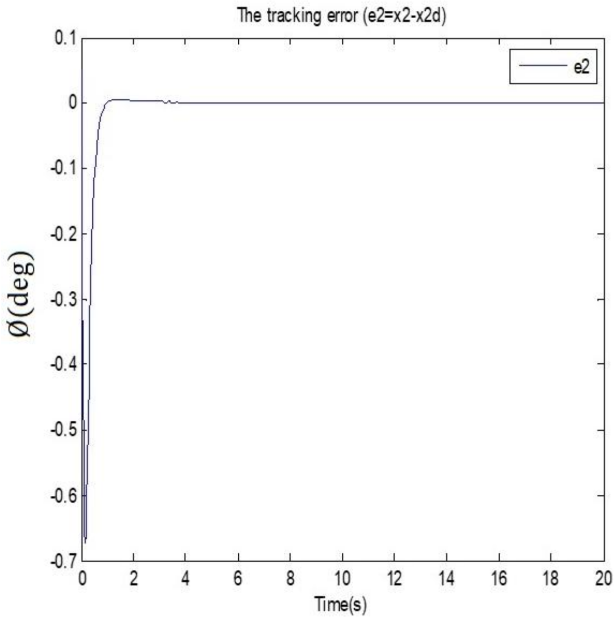

Fig. 5. Tracking errors e_2 evolution

The figures presenting the progression of tracking errors, rate angles, and roll angles are Figs. 2, 3 and 5, respectively, indicating the robustness and the satisfactory performance of the proposed control system in relation to the disturbance.

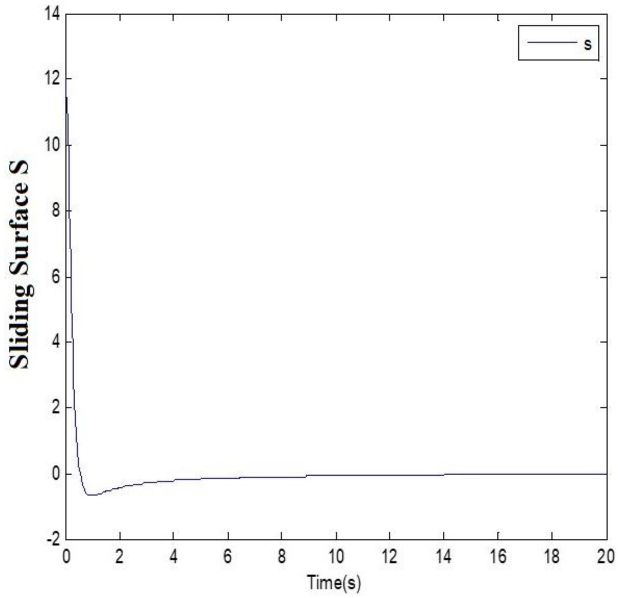

Fig. 6. Sliding surface *s* evolution

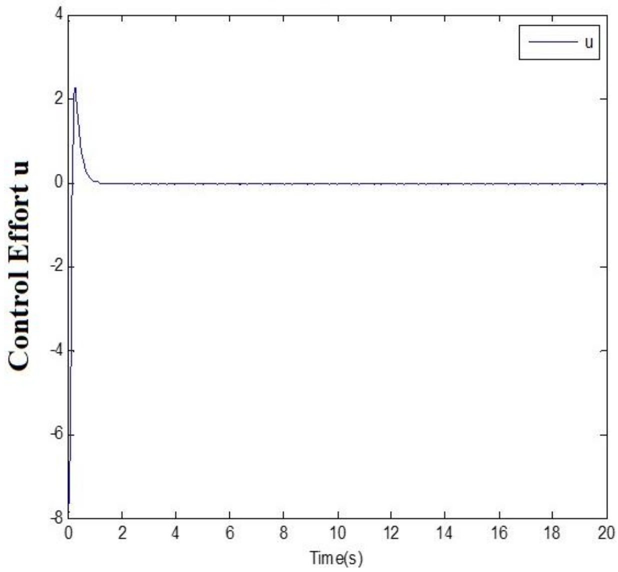

Fig. 7. Control law *u* evolution

Figure 7 demonstrated that the control law does not exhibit chattering. The evolution of the surface trajectory is shown in the Fig. 6. We notice that the system converges to zero and the attractiveness of the sliding surface.

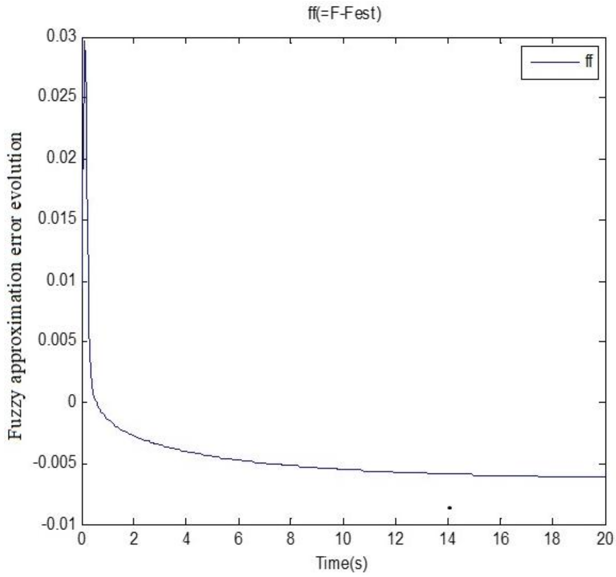

Fig. 8. Fuzzy approximation error evolution

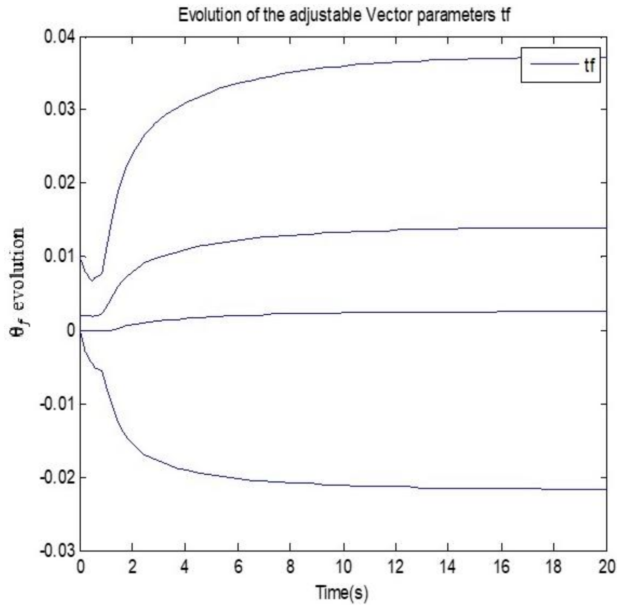

Fig. 9. θ_f evolution

Good approximation of the nonlinear function $f(x_1, x_2)$ is illustrated in Fig. 8. The convergence of θ_{f_i}, $i = 1, \ldots, 4$, and the behavior of adaptation parameters are presented in Fig. 9.

4.2. Case 2: a large initial condition

Figures 10–17 present the simulation results under the proposed controller.

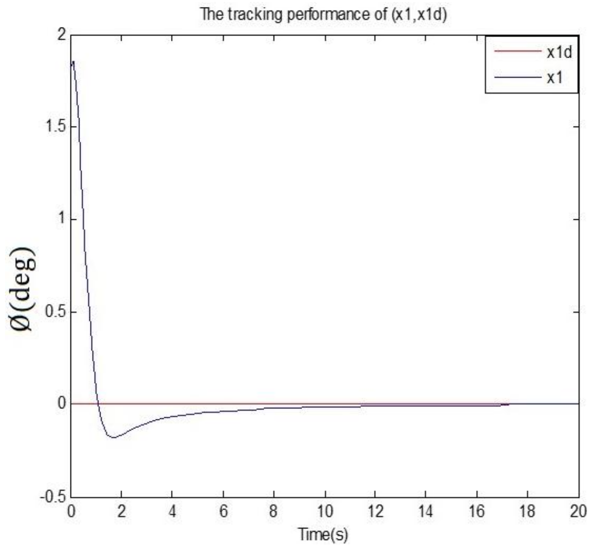

Fig. 10. Roll angle response $\phi(0) = 103.14°$, $\dot{\phi}(0) = 57.3°/s$

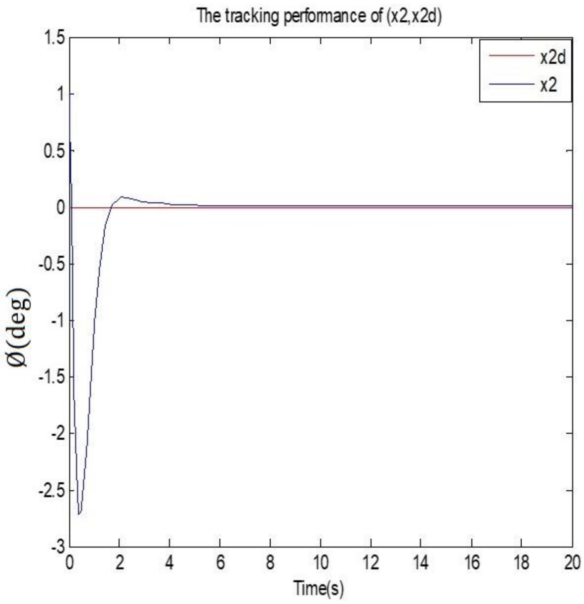

Fig. 11. Roll rate response $\phi(0) = 103.14°$, $\dot{\phi}(0) = 57.3°/s$

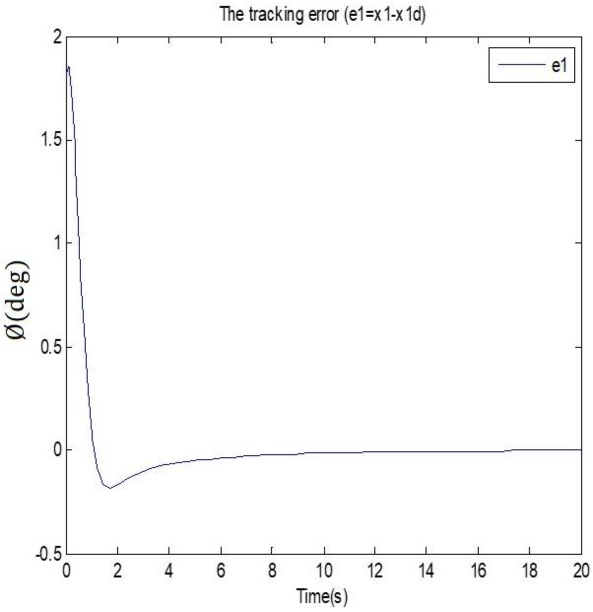

Fig. 12. Tracking errors e_1 $\phi(0) = 103.14°$, $\dot{\phi}(0) = 57.3°$/s evolution

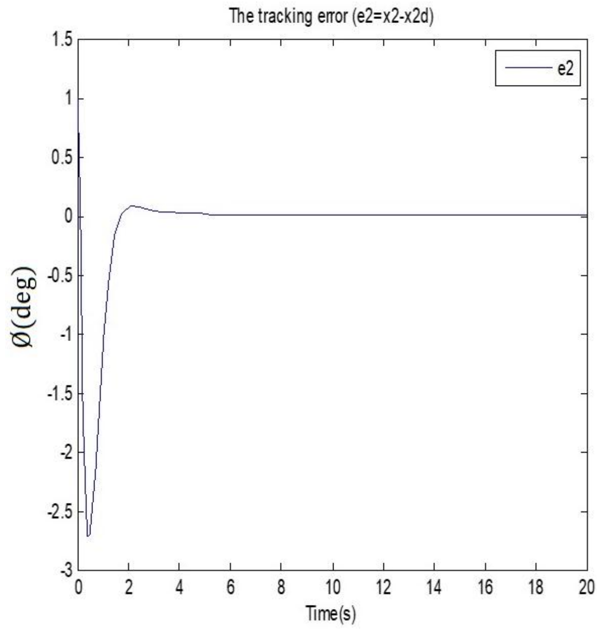

Fig. 13. Tracking errors e_2 $\phi(0) = 103.14°$, $\dot{\phi}(0) = 57.3°$/s evolution

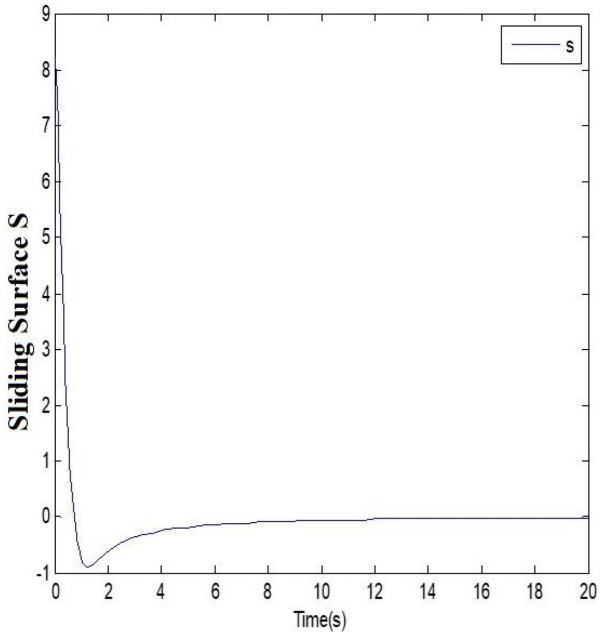

Fig. 14. Sliding surface s $\phi(0) = 103.14°$, $\dot{\phi}(0) = 57.3°$/s evolution

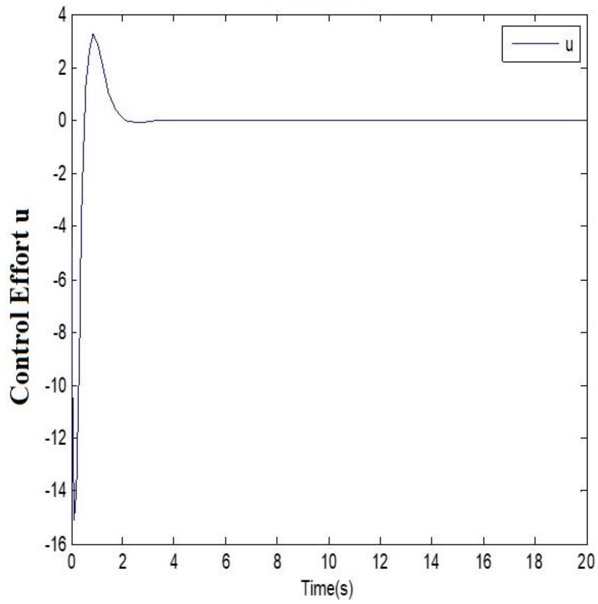

Fig. 15. Control law u $\phi(0) = 103.14°$, $\dot{\phi}(0) = 57.3°$/s evolution

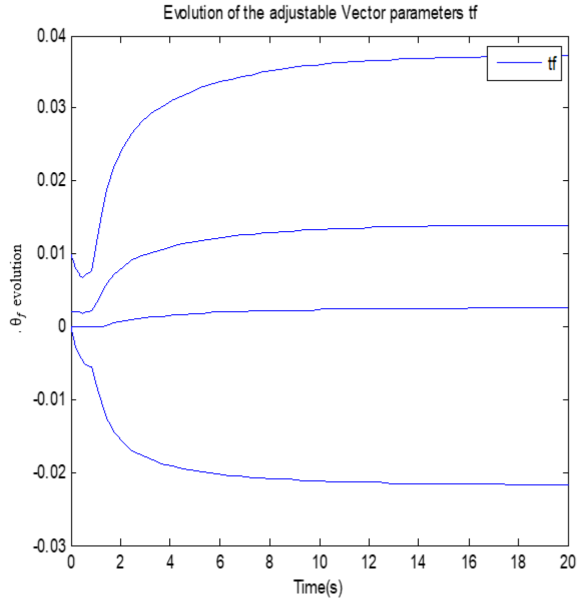

Fig. 16. θ_f $\phi(0) = 103.14°$, $\dot{\phi}(0) = 57.3°/s$ evolution

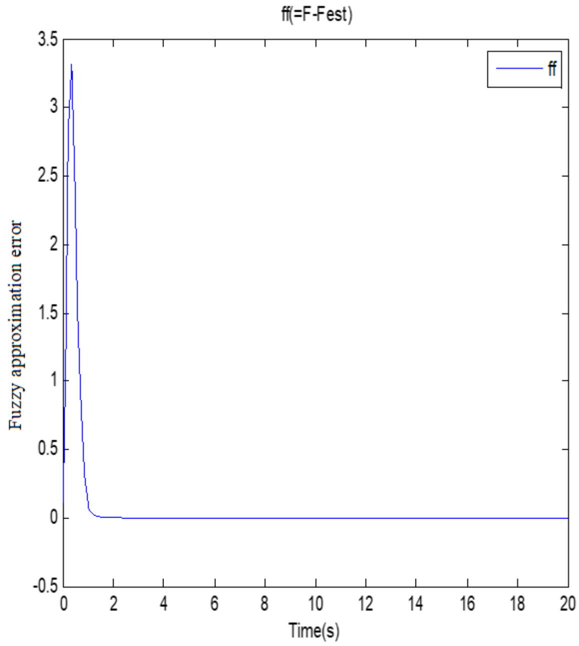

Fig. 17. Fuzzy approximation error $\phi(0) = 103.14°$, $\dot{\phi}(0) = 57.3°/s$ evolution

Figures 10 through 17 illustrate that the closed-loop responses are satisfactory, showcasing the controller's effective suppression and tracking capabilities across various initial conditions. The results reveal shorter settling times and better bounded signals compared to those outlined in [26]. Additionally, the dynamic function estimation is achieved with only 2 memberships for both states.

5. Comparative study

To demonstrate the effectiveness of the proposed approach, a comparative study is summarized in Table 2 and Table 3.

Table 2. Position case

	ESAFIS [26]	**RBF** [26]	**Proposed method**
Convergence time	5 s	7 s	4 s
Signal bounded	between 0 and 10	between (–40) and 40	between 0 and 0.2

Table 3. Velocity case

	ESAFIS [26]	**RBF** [26]	**Proposed method**
Convergence time	3 s	8 s	1 s
Signal bounded	between (–10) and 0	between (–80) and 80	between –0.7 and 0

After comparing the simulation results presented in Table 2 and Table 3, we confirm the efficiency of the proposed algorithm.

To illustrate the effectiveness of the proposed approach we consider the tracking problem. The selected reference trajectory vector is $[\boldsymbol{\phi_d}\ \boldsymbol{\dot\phi_d}]^T = [\mathbf{sin}(t)\ \mathbf{cos}(t)]^T$.

As shown in Figs. 18–19, under the normal sea conditions, the control method is robust and can ensure the tracking performance.

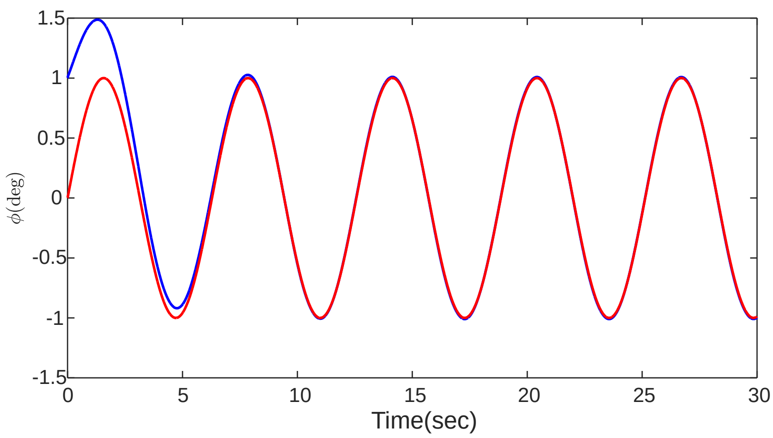

Fig. 18. Roll angle response

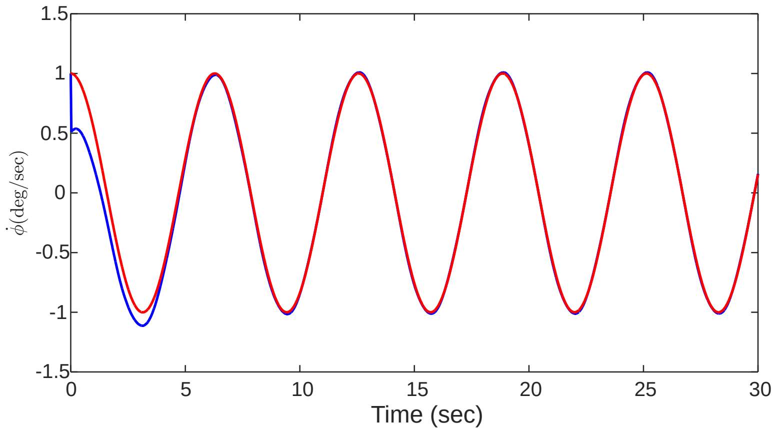

Fig. 19. Roll rate response

6. Conclusions

An adaptive moving fuzzy sliding mode tracking control approach was proposed to suppress wing rock phenomena and track the desired trajectories. In fact, nonlinear dynamics of the WRM system were considered time-varying uncertainties in this study. The online adjustment of the center and membership functions utilized to approximate the nonlinear dynamic function is our main contribution. The simulation results for various initial conditions for aircraft wing-rock motion show the efficacy of the suggested control approach. In future work, we are interested in exploring the feasibility of an optimization problem to address the significant number of adjustable parameters and compensate for the effects of fuzzy approximation errors.

Acknowledgements

The authors extend their appreciation to the Deputyship for Research & Innovation, Ministry of Education in Saudi Arabia for funding this research work through the project number RI-44-0226.

References

[1] Guo Y., Luo L., Bao C., *Design of a Fixed-Wing UAV Controller Combined Fuzzy Adaptive Method and Sliding Mode Control*, Mathematical Problems in Engineering, vol. 2022, no. 2812671 (2022), DOI: 10.1155/2022/2812671.

[2] Li D., Tsourdos A., Wang Z., Ignatyev D., *Nonlinear Analysis for Wing-Rock System with Adaptive Control*, Journal of Guidance, Control, and Dynamics, vol. 11, pp. 2174–2181 (2022), DOI: 10.2514/1.G006775.

[3] Wu D., Chen M., Gong H., Wu Q., *Robust backstepping control of wing rock using disturbance observer*, Applied Sciences, vol. 7, no. 3, 219 (2017), DOI: 10.3390/app7030219.

[4] Tavoosi J., *A new type-2 fuzzy sliding mode control for longitudinal aerodynamic parameters of a commercial aircraft*, Journal Européen des Systèmes Automatisés, vol. 53, no. 4, pp. 479–485 (2020), DOI: 10.18280/jesa.530405.

[5] Deng Z., Wu L., You Y., *Modeling and design of an aircraft-mode controller for a fixed-wing VTOL UAV*, Mathematical Problems in Engineering, vol. 2021, pp. 1–17 (2021), DOI: 10.1155/2021/7902134.

[6] Aljohani A.J., Mehedi I.M., Bilal M., Mahmoud M., Meem R.J., Iskanderani A.I., Alam M.M., Alasmary W., *Rotary flexible joint control using adaptive fuzzy sliding mode scheme*, Computational Intelligence and Neuroscience, vol. 2022 (2022), DOI: 10.1155/2022/2613075.

[7] Hemza M., *Robust adaptive control of coaxial octorotor UAV using type-1 and interval type-2 fuzzy logic systems*, vol. 73, no. 4, pp. 158–170 (2018), DOI: 10.18280/ama_c.730405.

[8] Singh S.N., Yirn W., Wells W.R., *Direct adaptive and neural control of wing-rock motion of slender delta wings*, Journal of Guidance, control, and Dynamics, vol. 18, no. 1, pp. 25–30 (1995), DOI: 10.2514/3.56652.

[9] Sreenatha A.G., Nair N.K., Sudhakar K., *Aerodynamic Suppression of Wing Rock Using Fuzzy Logic Control*, Journal of aircraft, vol. 37, no. 2, pp. 345–348 (2000), DOI: 10.2514/2.2602.

[10] Manring N.D., Muhi L., Fales R.C., Mehta V.S., Kuehn J., Peterson J., *Using Feedback Linearization to Improve the Tracking Performance of a Linear Hydraulic-Actuator*, J. Dyn. Sys., Meas., Control., vol. 1, no. 140, 011009 (2018), DOI: 10.1115/1.4037285.

[11] Howlader A.M., Urasaki N., Yona A., Senjyu T., Saber A.Y., *Design and Implement a Digital H∞ Robust Controller for a MW-Class PMSG-Based Grid-Interactive Wind Energy Conversion System*, vol. 4, no. 6, pp. 2084–2109 (2013), DOI: 10.3390/en6042084.

[12] Damani A.Y., Benselama Z.A., Hedjar R., *Formation control of nonholonomic wheeled mobile robots using adaptive distributed fractional order fast terminal sliding mode control*, Archive of Mechanical Engineering, vol. 70, no. 4, pp. 567–587 (2023), DOI: 10.24425/ame.2023.148700.

[13] Shin Y.H., *Adaptive Control System Designs for Aircraft Wing Rock*, vol. 39, no. 8, pp. 725–734 (2011), DOI: 10.5139/JKSAS.2011.39.8.725.

[14] Monahemi M.M., Krstic M., *Control of wing rock motion using adaptive feedback linearization*, Journal of Guidance, Control, and Dynamics, vol. 19, no. 4, pp. 905–912 (1996), DOI: 10.2514/3.21717.

[15] Guo Y., Luo L., Bao C., *Design of a Fixed-Wing UAV Controller Combined Fuzzy Adaptive Method and Sliding Mode Control*, Mathematical Problems in Engineering, vol. 2022 (2022), DOI: 10.1155/2022/2812671.

[16] Larguech S., Aloui S., Pagès O., El Hajjaji A., Chaari A., *Adaptive type-2 fuzzy sliding mode control for MIMO nonlinear systems: application to a turbocharged diesel engine*, in 2015 23rd Mediterranean Conference on Control and Automation (MED) (2015), DOI: 10.1109/MED.2015.7158751.

[17] Delmotte F., Hadj Taieb N., Hammami M.A., Meghnafi H., *An observer design for Takagi-Sugeno fuzzy bilinear control systems*, Archives of Control Sciences, vol. 33, no. 3, pp. 631–649 (2023), DOI: 10.24425/acs.2023.146959.

[18] Echreshavi Zeinab, Mohsen Farbood, Mokhtar Shasadeghi, Saleh Mobayen, *Reliable fuzzy control of uncertain nonlinear networked systems under actuator faults*, ISA transactions 141, pp. 157–166 (2023), DOI: 10.1016/j.isatra.2023.07.007.

[19] Nafia N., El Kari A., Ayad H., Mjahed M., *Robust full tracking control design of disturbed quadrotor UAVs with unknown dynamics*, Aerospace, vol. 5, no. 4, p. 115 (2018), DOI: 10.3390/aerospace5040115.

[20] Baklouti F., Aloui S., Chaari A., *Adaptive Fuzzy Sliding Mode Tracking Control of Uncertain Underactuated Nonlinear Systems*, Journal of Control Science and Engineering, vol. 2016, p. 6 (2016), DOI: 10.1155/2016/9283103.

[21] Farbood Mohsen, Mokhtar Shasadeghi, Taher Niknam, Behrouz Safarinejadian, Afshin Izadian, *Cooperative H∞ Robust Move Blocking Fuzzy Model Predictive Control of Nonlinear Systems*, IEEE Transactions on Systems, Man, and Cybernetics: Systems (2023), DOI: 10.1109/TSMC.2023.3299283.

[22] Farbood Mohsen, Zeinab Echereshavi, Mokhtar Shasadeghi, Saleh Mobayen, Paweł Skruch, *Disturbance Observer-based Data Driven Model Predictive Tracking Control of Linear Systems*, IEEE Access (2023), DOI: 10.1109/ACCESS.2023.3305496.

[23] Larguech S., Aloui S., Pagès O., El Hajjaji A., Chaari A., *Fuzzy sliding mode control for turbocharged diesel engine*, Journal of Dynamic Systems, Measurement, and Control, vol. 138, 011009 (2016), DOI: 10.1115/1.4031913.

[24] Shen Hao, Yun Wang, Jing Wang, Ju H. Park., *A Fuzzy-Model-Based Approach to Optimal Control for Nonlinear Markov Jump Singularly Perturbed Systems: A Novel Integral Reinforcement Learning Scheme*, IEEE Transactions on Fuzzy Systems (2023), DOI: 10.1109/TFUZZ.2023.3265666.

[25] Echreshavi Zeinab, Mohsen Farbood, Mokhtar Shasadeghi, *Disturbance observer-based fuzzy event-triggered ISMC design: Tracking performance*, ISA Transactions 138, pp. 243–253 (2023), DOI: 10.1016/j.isatra.2023.03.014.

[26] Rong H.J., Han S., Zhao G.S., *Adaptive fuzzy control of aircraft wing-rock motion*, Applied Soft Computing, vol. 14, pp. 181–193 (2014), DOI: 10.1016/j.asoc.2013.03.001.